1. THEORETICAL BACKGROUND AND EXPERIMENTAL TECHNIQUES

The number of transistors per chip grows exponentially in time, a trend now known as Moore's law [1]. In the next decades the size of semiconductors devices will shrink below 20 nm, where it is expected that quantum effects will become important. This is the reason why quantum information processing and its experimental implementation is a hot scientific topic nowadays. Its advantages over the classical information processing will be briefly reviewed.
Since the experimental technique most used in this work is electron spin resonance (ESR) its theoretical foundations are given. Additionally some of the basic pulse ESR and ENDOR experiments are also presented.

1.1 History of Quantum Computation

The idea to use a quantum mechanical system as a Turing machine was first proposed by Paul Benioff in 1980 [2], but his model of computation was purely classical. In 1982 Richard Feynman [3] suggested that a real physical (quantum) system cannot be fully simulated by any usual (classical) computer and that another quantum system might be used for the simulation. This conjecture appears to be valid, as was shown by Seth Lloyd in 1996 [4]. Meanwhile in 1985 David Deutsch [5] defined a quantum computer as a set of two level subsystems called quantum bits (qubits). He defined the universal quantum computer in analogy with the classical computer as composed of universal Turing machines and showed that the former is exponentially faster for certain problems than the latter because of the so called quantum parallelism. Later he developed a theory of quantum networks [6] and introduced quantum gates in analogy to classical logic gates. In 1992 Deutsch and Richard Jozsa [7] presented a first algorithm that uses quantum parallelism for a specific problem, but the problem described there has no practical application.
The real breakthrough in theory came in 1994 when Peter Shor introduced his algorithm for factorizing numbers [8, 9], which is exponentially faster than any classical algorithm for large numbers. This result drew attention to the subject, because nowadays every protocol for secure communication (e.g. electronic bank transfer)

relies on the fact that very large numbers cannot be factorized in reasonable time. For classical computation, the time needed for factorizing grows exponentially with the number of digits, while Shor's quantum algorithm is only polynomial in time. Another important algorithm was found in 1997 by Lov K. Grover [10]. He showed that for a database with N unsorted entries (like the phone numbers in a phone book), a quantum computer will find a record of interest with probability 0.5 making $O(\sqrt{N})$ accesses, while a classical computer needs $N/2$ searches. The advantages of quantum computers became more obvious.
Despite the fast development of theory, experimental implementation of quantum computation is very difficult and until today there are only proof-of-principle experiments. There are many proposals to build a quantum computer based on different physical systems like ion traps [11], cavity quantum electrodynamics [12], Josephson junctions and superconducting loops [13, 14], quantum dots [15], nuclear spins coupled to one electron spin 1/2 (S-Bus concept) [16] and endohedral fullerenes [17, 18, 19]. The last approach will be discussed later in more detail, as it is connected to this work. The most successful demonstration of quantum computation until now is based on ensembles of nuclear spins and uses state of the art Nuclear Magnetic Resonance (NMR) technology [20, 21]. It consists of an application of Shor's algorithm to factorize 15 (finding that $15 = 5 \times 3$) [22]. This result is of course trivial, but it shows that a quantum computer can really work. Unfortunately the used liquid NMR implementation is not scalable [23], meaning that it will not work for more then 20-40 qubits (the quantum bits, see section 1.2) while at least a few hundred are needed in order to gain a significant advantage over classical computers.

1.2 Qubits

In a classical computer (or any digital electronic device), the information is stored and processed in binary units called bits. In a computer memory for example the bits are physically realized as small capacitors - a charged capacitor corresponds to logical "one" and an empty one to logical "zero". The bit is always in one of both states (a partially charged capacitor is a faulty bit). In a quantum computer the information is processed by qubits where zero is denoted by $|0\rangle$, one by $|1\rangle$. For a example when the qubits are spin 1/2 particles (electrons or nuclei) then usually spin-up means zero and spin-down means one (for the definition of "spin-up" and "spin-down" see section (1.4.1)). The peculiar property of the qubits that distinguishes them from classical bits is that they can be simultaneously "zero" and

"one". Such a superposition state is expressed mathematically as:

$$|\psi\rangle = a|0\rangle + b|1\rangle \tag{1.1}$$

where a and b are complex numbers. The probability of the qubit to be measured in state $|0\rangle$ is a^2 and in state $|1\rangle$ b^2, and the normalization condition $a^2 + b^2 = 1$ has to be fulfilled. The states $|0\rangle$ and $|1\rangle$ form a basis in a Hilbert space with 2 dimensions, where the state of the qubit is represented as a vector with components a and b. For N qubits $|\psi\rangle_1$, $|\psi\rangle_2$, ... $|\psi\rangle_N$ (N two level systems) the Hilbert space is constructed as a tensor product between single qubit spaces $|\psi\rangle_1 \otimes |\psi\rangle_2 \otimes ...|\psi\rangle_N$, it has 2^N dimensions and correspondingly 2^N states basis.
Logic operations on qubits are described by quantum logic gates which correspond to unitary transformations U in Hilbert space. An important single qubit operation is the NOT-gate with matrix representation:

$$U_{NOT} = \begin{pmatrix} 0 & 1 \\ 1 & 0 \end{pmatrix}$$

If the initial state of the qubit is $|0\rangle$, the NOT-gate changes it to $|1\rangle$:

$$\begin{pmatrix} 0 & 1 \\ 0 & 1 \end{pmatrix} \begin{pmatrix} 1 \\ 0 \end{pmatrix} = \begin{pmatrix} 0 \\ 1 \end{pmatrix}$$

If the qubit is in a general state as described by equation (1.1), the NOT-gate exchanges the probabilities a^2 and b^2 to find the system in the states $|0\rangle$ and $|1\rangle$:

$$\begin{pmatrix} 0 & 1 \\ 1 & 0 \end{pmatrix} |\psi\rangle = \begin{pmatrix} b \\ a \end{pmatrix} = b|0\rangle + a|1\rangle$$

The NOT operation is a special case of single qubit rotation (see section 1.5.3) at angle π. For two qubits there are $2^2 = 4$ basis states in Hilbert space, so the state of the system is given by:

$$|\psi\rangle = c_0|0\rangle + c_1|1\rangle + c_2|2\rangle + c_3|3\rangle$$

which is usually written as:

$$|\psi\rangle = c_0|00\rangle + c_1|01\rangle + c_2|10\rangle + c_3|11\rangle \tag{1.2}$$

In case of spins as qubits, equation (1.2) is sometimes written:

$$|\psi\rangle = c_0|\uparrow\uparrow\rangle + c_1|\uparrow\downarrow\rangle + c_2|\downarrow\uparrow\rangle + c_3|\downarrow\downarrow\rangle \tag{1.3}$$

where $|\uparrow\rangle$ means "spin-up" and $|\downarrow\rangle$ "spin-down".
Among all possible two-qubit quantum gates, the controlled-NOT (CNOT) gate deserves special attention, because it is a universal gate. This means that any (two qubit) gate can be constructed from a finite number of CNOT gates and single qubit rotations [24]. The input qubits to which this gate is applied are called control qubit and target qubit. When the initial state of the control qubit is $|0\rangle$, the target qubit is left unaltered, and when it is $|1\rangle$, the target is inverted (a NOT operation is applied). The matrix form of the CNOT operation is:

$$U_{CNOT} = \begin{pmatrix} 1 & 0 & 0 & 0 \\ 0 & 1 & 0 & 0 \\ 0 & 0 & 0 & 1 \\ 0 & 0 & 1 & 0 \end{pmatrix} \tag{1.4}$$

If we write the basis vectors for the two qubit Hilbert space like this:

$$|\downarrow\downarrow\rangle \equiv \begin{pmatrix} 1 \\ 0 \\ 0 \\ 0 \end{pmatrix}; |\downarrow\uparrow\rangle \equiv \begin{pmatrix} 0 \\ 1 \\ 0 \\ 0 \end{pmatrix}; |\uparrow\downarrow\rangle \equiv \begin{pmatrix} 0 \\ 0 \\ 1 \\ 0 \end{pmatrix}; |\uparrow\uparrow\rangle \equiv \begin{pmatrix} 0 \\ 0 \\ 0 \\ 1 \end{pmatrix};$$

and apply U_{CNOT} to the last two states (it does not affect the first two):

$$U_{CNOT}|\uparrow\downarrow\rangle \equiv U_{CNOT} \begin{pmatrix} 0 \\ 0 \\ 1 \\ 0 \end{pmatrix} = \begin{pmatrix} 0 \\ 0 \\ 0 \\ 1 \end{pmatrix} \equiv |\uparrow\uparrow\rangle$$

$$U_{CNOT}|\uparrow\uparrow\rangle \equiv U_{CNOT} \begin{pmatrix} 0 \\ 0 \\ 0 \\ 1 \end{pmatrix} = \begin{pmatrix} 0 \\ 0 \\ 1 \\ 0 \end{pmatrix} \equiv |\uparrow\downarrow\rangle$$

Here the first bit is the control qubit and second one is the target.

1.3 Entanglement

Two coupled two level systems (spins, photons) have very striking properties which led Einstein, Podolsky and Rosen (EPR) [25] to claim that the description of quantum mechanics with a wave function is incomplete. In a later paper [26] Niels Bohr argued that we cannot deny the success of quantum theory and that the authors should reconsider what they called "physical reality". The same argument was also made by Erwin Schrödinger [27], who introduced the term entanglement (Verschränkung). Despite those discussions there was a lack of mathematical definition of the problem until it was given by Bell in 1964 [28] who derived what are now called Bell's inequalities. The latter were proven experimentally (with photons for example [29] and protons [30]) to be violated, confirming that quantum mechanics is correct and all "local realistic theories" are invalid.
Two spin 1/2 particles as an example will be considered, following [31]. They can be prepared in the following state:

$$|\psi\rangle = \frac{1}{\sqrt{2}}(|\uparrow\downarrow\rangle + |\downarrow\uparrow\rangle) \tag{1.5}$$

After their preparation the particles are let to move in opposite directions and then each of them passes a Stern-Gerlach set-up A and B to measure its spin. If set-up A has the z-axis as quantization axis (S_z is measured) and the passing particle in measured to be in the "spin-up" state, then the other one must be in "spin-down" state according to eq. (1.5) if S_z is measured. However, if set-up B measures S_x, then it will give "spin-up" and "spin-down" with probability 1/2. So it seems that the result of the measurement from B depends on which quantization axis in chosen in A - x or z. The quantum-mechanical interpretation of this paradox is simply that the two electrons are still one system, even if they are spatially separated. The state (1.5) is called an entangled or Bell state. It is the "heart" of all quantum algorithms and quantum cryptography protocols.

1.4 Electron Spin Resonance (ESR)

The method of Electron Spin Resonance (ESR)[1], first discovered by Zavoiskii [32], has found wide application in biology, chemistry and physics. As this is the experimental method mostly used in this work, its basics will be discussed briefly.
The general spin Hamiltonian for a system consisting of electron and nuclear spins

[1] A frequently used term is Electron Paramagnetic Resonance (EPR), but Electron Spin Resonance (ESR) is recently used more often in order not to confuse it with the EPR from section 1.3

is usually given by:

$$H = H_{ZI} + H_{ZFS} + H_{HI} + H_{NZI} + H_{NQI} \tag{1.6}$$

where H_{ZI}, H_{ZFS}, H_{HI}, H_{ZI} and H_{NQI} are correspondingly the Zeeman interaction, zero field splitting (fine structure) interaction, hyperfine interaction, nuclear zeeman interaction and nuclear quadrupole interaction Hamiltonians. The last two terms in equation (1.6) will be neglected because their contribution to the Hamiltonian is much smaller in endohedral fullerenes (the systems studied here) than that of the other terms. The latter will be described in the following sections.

1.4.1 Zeeman Interaction and continuous wave ESR

The Hamiltonian of an electron spin in constant applied magnetic field (Zeeman interaction) can be written as [33]:

$$H_{ZI} = \hbar\omega_0 S_z, \quad \omega_0 = \gamma_e B_0 = \frac{g\mu_B}{\hbar} B_0 \tag{1.7}$$

here $\hbar$ is Planck's constant divided by 2π, ω_0 is the Larmor frequency, B_0 is the constant magnetic field applied parallel to the z-axis, g is the Landé factor (generally a second-rank tensor, but for the systems investigated in this work it is found to be always isotropic), μ_B is the Bohr magneton and S_z is the z electron spin operator:

$$S_z = \begin{pmatrix} \frac{1}{2} & 0 \\ 0 & -\frac{1}{2} \end{pmatrix}$$

The electron is in the "spin-up" state when its projection onto the z-axis is positive (parallel to the magnetic field) and "spin-down" when it is negative (anti-parallel to B_0). Using the states $|\frac{1}{2}\rangle$ ($|\uparrow\rangle$) and $|-\frac{1}{2}\rangle$ ($|\downarrow\rangle$) as a basis in Hilbert space, we can calculate the energies for both orientations:

$$\langle \pm\frac{1}{2}|H|\pm\frac{1}{2}\rangle = \hbar\omega_0 \langle \pm\frac{1}{2}|S_z|\pm\frac{1}{2}\rangle = \pm\frac{1}{2}\hbar\omega_0 \tag{1.8}$$

It is clear that a photon with energy $E = \hbar\omega_0$ can be absorbed by a spin in the $|-1/2\rangle$ state and this is basically the phenomenon of ESR. If there is more than one unpaired electron, the total spin is M_S and the quantum number is $m_S = -M_S, -M_S+1, ..., +M_S$, i.e. we have $2M_S+1$ energy states:

$$\langle m|H|n\rangle = \hbar\omega_0 \langle m|S_z|n\rangle = m_S \hbar\omega_0 \delta_{mn} \tag{1.9}$$

where δ_{mn} is Kronecker's symbol. Applying the selection rule in ESR $\Delta m_S = \pm 1$, there are $2M_S$ allowed transitions (all with the same energy if there is no ZFS, see the next section).
The energy of the transitions are in the microwave (MW) region, usually about 9.4 GHz ($B_0 \approx 0.336\ T$ for $g \approx 2.002$) called X-Band. Other often used frequencies are L-Band (2 GHz, $B_0 = 0.071\ T$), Q-band (34 GHz, $B_0 = 1.21\ T$) and W-band (94 GHz, $B_0 = 3.36\ T$).
Experimentally it is very difficult to change the MW frequency continuously and over a wide range. Therefore the latter is held constant and the applied magnetic field is swept, which can be more easily achieved. This type of experiments are called continuous wave (CW) ESR and they are more often used than the pulsed ESR, which will be discussed in more detail in section 1.5.

1.4.2 Zero Field Splitting (Fine Structure)

For a system with an electron spin quantum number $M_S > \frac{1}{2}$, an additional splitting of the ESR spectral lines called zero field splitting (ZFS) or fine structure can occur if the symmetry of the system is lower than cubic. The ZFS is described by the second term in the spin Hamiltonian (1.6):

$$H_{ZFS} = \mathbf{S^t}.\mathbf{D}.\mathbf{S} \tag{1.10}$$

where

$$\mathbf{S} = \begin{pmatrix} S_x \\ S_y \\ S_z \end{pmatrix} \tag{1.11}$$

is the electron spin operator $\mathbf{S}$ in vector form with components S_x, S_y and S_z; $\mathbf{S^t}$ is the transpose of $\mathbf{S}$, and $\mathbf{D}$ is a second-rank tensor characterizing the interaction, which in appropriate basis has the form:

$$\mathbf{D} = \begin{pmatrix} -\frac{1}{3}D + E & 0 & 0 \\ 0 & -\frac{1}{3}D - E & 0 \\ 0 & 0 & \frac{2}{3}D \end{pmatrix} \tag{1.12}$$

depending on the two scalar parameters D and E given in MHz or Gaussian units. The energy levels for $M_S = \frac{3}{2}$ will be given explicitly, as they are needed for later discussions. The parameter E will be neglected, because it is absent or much smaller than D for the systems considered in this work. Now the D matrix (1.12) and the

Hamiltonian (1.10) are simplified and can be written as [34]:

$$H_{ZFS} = D(S_z^2 - \frac{1}{3}M_S(M_S+1)) \tag{1.13}$$

If the the applied magnetic field is not parallel to the z-axis, but at an angle θ in the xz-plane, the spin Hamiltonian is:

$$H = H_{ZI} + H_{ZFS} = \hbar\omega_0(\cos\theta S_z + \sin\theta S_x) + D(S_z^2 - \frac{1}{3}M_S(M_S+1)) \tag{1.14}$$

with eigenvalues (for $D << \hbar\omega_0$):

$$\begin{aligned} E_{\pm\frac{1}{2}} &= \pm\frac{1}{2}\hbar\omega_0 - \frac{1}{2}D(3\cos^2(\theta)-1) \\ E_{\pm\frac{3}{2}} &= \pm\frac{3}{2}\hbar\omega_0 + \frac{1}{2}D(3\cos^2(\theta)-1) \end{aligned}$$

The energy levels are non-degenerate even if there is no magnetic field applied, which is why this interaction is called zero-field splitting. The resonant fields of the corresponding allowed transitions are:

$$B_0^{(+\frac{3}{2},+\frac{1}{2})} = \frac{h\nu_{MW}}{g\mu_B} - D(3\cos^2(\theta)-1) \tag{1.15}$$

$$B_0^{(+\frac{1}{2},-\frac{1}{2})} = \frac{h\nu_{MW}}{g\mu_B} \tag{1.16}$$

$$B_0^{(-\frac{1}{2},-\frac{3}{2})} = \frac{h\nu_{MW}}{g\mu_B} + D(3\cos^2(\theta)-1) \tag{1.17}$$

where $B_0^{\frac{3}{2}\frac{1}{2}}$, $B_0^{+\frac{1}{2}-\frac{1}{2}}$ and $B_0^{-\frac{1}{2}-\frac{3}{2}}$ are the resonance fields at which each of the lines appear and ν_{MW} is the constant MW frequency. From the equations above it clear that for a single crystal sample, the position of two of the ESR lines will depend on the sample orientation with respect to the B_0 field as $(3\cos^2(\theta)-1)$, with maximum separation $2D$ for $\theta = 0$. For the "magic angle" $\theta \approx 54.7°$ all lines collapse in one.

1.4.3 Hyperfine Interaction

If there is a nuclear spin with spin quantum number M_I coupled to the electron spin, a hyperfine interaction is present described by the term H_{HI} in the spin Hamiltonian (1.6):

$$H_{HI} = \mathbf{S}.\mathbf{A}.\mathbf{I} \tag{1.18}$$

where $\mathbf{S}$ and $\mathbf{I}$ are the electron and nuclear spin operators and $\mathbf{A}$ is a second-rank tensor. If the hyperfine interaction is isotropic, as it is for the endohedral fullerenes

considered in this work, Eq. (1.18) becomes:

$$H_{HI} = \hbar\, 2\pi a\, \mathbf{S.I} = \hbar\, 2\pi a(S_x I_x + S_y I_y + S_z I_z) \tag{1.19}$$

Here, the factor 2π is written explicitly so that the isotropic hyperfine constant a is expressed in frequency units. The number of spectral lines is (in the general case of non-vanishing zero-field splitting) $2M_S(2M_I+1)$, for example for one electron ($M_S = \frac{1}{2}$) coupled to one nuclear spin with $M_I = \frac{1}{2}$ there are two allowed transitions and correspondingly two spectral lines.

1.4.4 Line Shapes

Magnetic resonance does not occur at only one value of the field, but there is a certain distribution of the MW absorption around it. Experimentally, the absorption is not directly recorded but its first derivative, as this tremendously increases the sensitivity. Afterwards the signal has to be integrated to obtain the absorption spectral line. Usually two absorbtion line shapes are considered - Lorentzian and Gaussian. The two line shape functions are:

$$g_L(B) = \frac{A_0}{1 + a^2(B_0 - B)^2}$$

for the Lorentzian and

$$g_G(B) = A_0 e^{-b^2(B_0-B)^2}$$

for the Gaussian. There are two types of line broadening - homogeneous and inhomogeneous (see for example [34, 35]). Possible sources for the first type are dipolar interaction between like spins, spin-lattice relaxation (characterized by T_1), interaction with the radiation field and spectral diffusion. The shape of a homogeneously broadened line is Lorentzian. Multiple homogeneously broadened lines build the envelope of an inhomogeneously broadened line with Gaussian, Lorentzian or Voigt line shape. The latter is a combination of the first two types and is often used to explain experimentally observed line shapes that cannot be described by the former two. The inhomogeneous broadening can be caused by inhomogeneities of the applied magnetic field, unresolved fine and hyperfine structure, dipolar interactions between unlike spins, and crystal defects.
An important property of the spectral line is its width, often defined as full width at half height (FWHH) $\Delta B_{1/2}$. This is the width of the line at $g(B) = A_0/2$. For a

Lorentzian line $\Delta B_{1/2} = 2/a$ and for a purely homogeneously broadened line:

$$\Delta B_{1/2} = \frac{2\hbar}{g\mu_B T_2} \tag{1.20}$$

where T_2 is the spin-spin relaxation time. For an inhomogeneously broadened line instead of T_2, a T_2^* is defined. The line width is often used to calculate relaxation times but the latter are more precisely measured with pulsed ESR. This method will be described in the next section and relaxation is presented later in more detail in section 1.5.6 and chapter 4.

1.5 Pulsed ESR

In this section the basics of pulsed EPR will be presented briefly, as this is the experimental technique most widely used in this work.

1.5.1 Classical Picture

When an ensemble of electron spins is put in a constant magnetic field, it possesses a net magnetization M_0 that precesses with the Larmor frequency ω_0 eq. (1.7) around the field axis (z axis). If additionally microwave radiation is applied with magnetic field magnitude B_1 then M_0 will precess also around B_1. To simplify this complicated movement, a rotating frame of reference is defined, instead of the laboratory frame, which rotates with angular frequency ω_0 around z and in most experiments B_1 is chosen perpendicular to z. If, for example, B_1 is parallel to the y axis, then correspondingly M_0 rotates around y, because of the Lorentz force, with the Rabi frequency:

$$\omega_1 = \frac{g\mu_B B_1}{\hbar} \tag{1.21}$$

Usually the radiation is in form of a pulse with such a length that M_0 is rotated by a given angle according to the formula:

$$\beta = \omega_1 t_p \tag{1.22}$$

here β is the rotation angle in radians and t_p is the pulse length, typically 10-100 ns.

1.5.2 Pure and Mixed States. Density Matrix

When a quantum system is in a well defined state, as in the cases considered in the previous sections, then it is in a so-called pure state (e.g. an electron spin in the

$|\uparrow\rangle$ or "spin-up" state). Usually all experiments are performed using an ensemble of particles and not a single particle (there are exceptions like quantum dots and superconducting devices) and this complicates the physical picture. Let us consider an ensemble of electron spins. If put in a constant magnetic field, some of the spins will orient themselves with respect to the field direction and the other part will be aligned in the opposite direction because there is a Boltzmann distribution of level populations. The population difference gives rise to the net magnetization M_0 defined in the previous section. This is an example of a mixed state. For the quantum mechanical description of such states the density operator or density matrix is defined (for details see [36, 37]). For the two possible orientations of the electron spin as equation (1.1), the density matrix of this mixed state has the form:

$$\rho = |\psi\rangle\langle\psi| = \begin{pmatrix} aa^* & ab^* \\ a^*b & bb^* \end{pmatrix} \tag{1.23}$$

or:

$$\rho = aa^*|0\rangle\langle 0| + bb^*|1\rangle\langle 1| + a^*b|1\rangle\langle 0| + ab^*|0\rangle\langle 1|$$

Here the meaning of a and b is like in (1.1) and * is the complex conjugate. The diagonal elements of the density matrix aa^* and bb^* correspond to the probability of the system to be in state $|\uparrow\rangle$ or $|\downarrow\rangle$ state respectively. The off-diagonal elements measure the coherence between $|\uparrow\rangle$ and $|\downarrow\rangle$. For the density matrix the normalization condition should be fulfilled:

$$tr(\rho) = 1 \tag{1.24}$$

The expectation value of an observable M is:

$$\langle\psi|M|\psi\rangle = tr(\rho M) \tag{1.25}$$

If the quantum system is in a pure state, for example $|\uparrow\rangle$ then the density matrix 1.23 is simplified to:

$$\rho = \begin{pmatrix} aa^* & 0 \\ 0 & 0 \end{pmatrix}$$

All quantum algorithms assume that the qubits are initialized before the calculation, meaning that the system is in a pure state. However, for the experimental implementation such a pure state must be specifically prepared and usually this is

not simple. The concept of pseudo-pure states was introduced [20] for ensemble quantum computing in NMR.
It can be shown (see for example [37]) that for the density matrix of any mixed state (for example equation (1.23)) the following inequality holds:

$$tr(\rho^2) < 1 \tag{1.26}$$

and for a pure state (equation (1.26)):

$$tr(\rho^2) = 1$$

which can be used to test whether a given state is pure or not, and with what fidelity.

1.5.3 Liouville-von Neumann equation

The dynamics of mixed states described by the density matrix (if relaxation is neglected) is covered by the Liouville-von Neumann equation:

$$\frac{d\rho(t)}{dt} = -\frac{i}{\hbar}[H(t), \rho(t)] \tag{1.27}$$

with i the imaginary unit and $[,]$ commutator brackets. In pulsed ESR experiments, it is often possible to divide the time evolution into two segments - free evolution under time-independent Hamiltonian and evolution under pulse application. For the former Hamiltonian H the formal solution is:

$$\rho(t) = U\rho(0)U^\dagger = e^{-\frac{i}{\hbar}Ht}\rho(0)\, e^{\frac{i}{\hbar}Ht} \tag{1.28}$$

where U is a unitary transformation called propagator.
An ensemble of spins in a magnetic field is in thermal equilibrium according to the Boltzmann distribution. Its density matrix is:

$$\rho_B = \frac{e^{-\frac{H}{kT}}}{Tr(e^{-\frac{H}{kT}})} \tag{1.29}$$

where H is the spin Hamiltonian (1.6). Usually the Zeeman interaction dominates all other spin interactions and often $\frac{\hbar\omega_0}{kT} << 1$. The exponent can then be expanded in a series and to first order eq. (1.29) becomes:

$$\rho_B = \frac{\mathbb{1} - \frac{\hbar\omega_0}{kT}S_z}{Tr\left(\mathbb{1} - \frac{\hbar\omega_0}{kT}S_z\right)} = \frac{\mathbb{1}}{Tr\left(\mathbb{1}\right)} - \alpha S_z \tag{1.30}$$

Here, $\mathbb{1}$ is the identity operator, which is not influenced by unitary transformations. Proportional constants can be omitted as the experimental signal is in arbitrary units and must always be compared to a known spin standard. After these simplifications the Boltzmann density matrix is written in the high temperature approximation like:

$$\tilde{\rho}_B = S_z \tag{1.31}$$

A pulse applied to the spin ensemble can be described by the spin rotation propagator (eq. 1.28):

$$P_{x,y}(\beta) = e^{-i\beta S_{x,y}} \tag{1.32}$$

with i the imaginary unit, β the rotating angle and S_x and S_y the x and y electron spin operators, which for $S = 1/2$ look like:

$$S_x = \begin{pmatrix} 0 & \frac{1}{2} \\ \frac{1}{2} & 0 \end{pmatrix} \quad S_y = \begin{pmatrix} 0 & -\frac{i}{2} \\ \frac{i}{2} & 0 \end{pmatrix} \tag{1.33}$$

It is now worth noting that for spins as qubits the NOT operation is equivalent to a rotation about an angle π (π pulse applied).
The spin ensemble evolves when there is no pulse applied (free evolution) according to eq. 1.28 with the following propagator:

$$U_{evol} = e^{-\frac{i}{\hbar}Ht} \tag{1.34}$$

where the spin Hamiltonian is given by (1.6).

1.5.4 Liouville space

The Liouville space is a generalization of the n-dimensional Hilbert space and has n^2 dimensions [38, 39, 33]. This new superspace, as it is also called, is spanned by a basis of operators defined in Hilbert space and not by state vectors. The notation is simplified, because any observable and the density matrix itself are vectors in Liouville space, and processes such as relaxation can be described (see chapter 4 for more detail). The operators in the Liouville space are called superoperators and the propagators superpropagators. The Hilbert space of an electron spin 1/2 has two basis states, namely $|\uparrow\rangle$ and $|\downarrow\rangle$, while the corresponding superspace has 4 dimensions and a usual basis is given by the three spin operators and the identity operator. The basis is written as $|\mathbb{1})$, $|S_x)$, $|S_y)$ and $|S_z)$. The spin rotation operator (1.32) in Liouville space reads:

$$P_y(\beta) = e^{-i\beta\hat{\hat{S}}_y} \tag{1.35}$$

where $\hat{\hat{S}}_y$ is the superoperator relative to S_y. If the propagator (1.35) is applied to the thermal equilibrium state $\tilde{\rho_B} = |S_z)$, then [33]:

$$\begin{aligned} e^{-i\beta\hat{\hat{S}}_y}\tilde{\rho_B}e^{+i\beta\hat{\hat{S}}_y} &= |e^{-i\beta\hat{\hat{S}}_y}S_z e^{+i\beta\hat{\hat{S}}_y}) = \\ = |\cos(\beta)S_z + \sin(\beta)S_x) &= \cos(\beta)|S_z) + \sin(\beta)|S_x) \end{aligned} \tag{1.36}$$

For the free evolution of the system in Liouville picture the spin Hamiltonian in (1.34) should be replaced with $\hat{\hat{H}}$:

$$\hat{\hat{U}}_{evol} = e^{-\frac{i}{\hbar}\hat{\hat{H}}t} \tag{1.37}$$

The observable in magnetic resonance is the spin operator $S_+ = S_x + iS_y$ which corresponds to the quadrature detection in the (x,y) plane. According to equation (1.25) the signal can be calculated with:

$$S = Tr(\rho S_+) \tag{1.38}$$

1.5.5 Fictitious spin 1/2 operator formalism

For an electron spin $S > 1/2$ the corresponding spin operators in eq. (1.32) should be used. In the absence of ZFS, the transition frequencies are equal and the pulses have to be described with the full spin operators, which for $S = 3/2$ are written like:

$$S_z = \begin{pmatrix} \frac{3}{2} & 0 & 0 & 0 \\ 0 & \frac{1}{2} & 0 & 0 \\ 0 & 0 & -\frac{1}{2} & 0 \\ 0 & 0 & 0 & -\frac{3}{2} \end{pmatrix} \tag{1.39}$$

$$S_x = \frac{1}{2}\begin{pmatrix} 0 & \sqrt{3} & 0 & 0 \\ \sqrt{3} & 0 & 2 & 0 \\ 0 & 2 & 0 & \sqrt{3} \\ 0 & 0 & \sqrt{3} & 0 \end{pmatrix} \tag{1.40}$$

$$S_y = \frac{i}{2}\begin{pmatrix} 0 & -\sqrt{3} & 0 & 0 \\ \sqrt{3} & 0 & -2 & 0 \\ 0 & 2 & 0 & -\sqrt{3} \\ 0 & 0 & \sqrt{3} & 0 \end{pmatrix} \tag{1.41}$$

If zero-field splitting is present or if there are two or more coupled spins, the spectral lines can be so well separated that the simultaneous excitation of all of them is either impossible or undesirable. In this case a MW pulse can selectively excite one

transition and may not affect the neighboring ones. For a simpler description in these cases the so called fictitious or effective spin 1/2 operator formalism [40, 41] is defined. The basic idea is merely to assign to every allowed transition the three usual spin 1/2 operators S_x, S_y, S_z. For a spin S the matrices of the spin operators have $(2S+1)(2S+1)$ elements. The fictitious operators have the same number of elements, but all of them are zero except the ones that connect the states of the corresponding allowed transition. As an example we consider an electron spin system as the group V endohedral fullerenes with $S = 3/2$ and $S_{x,y,z}$ from equation (1.39) but for simplicity without coupled nuclear spins ($I = 0$). There are three allowed transitions: $|+3/2\rangle \leftrightarrow |+1/2\rangle$, $|+1/2\rangle \leftrightarrow |-1/2\rangle$ and $|-1/2\rangle \leftrightarrow |-3/2\rangle$. For everey one of them a set of the three usual spin operators is introduced. For example for the transition $|+3/2\rangle \leftrightarrow |+1/2\rangle$ the spin operators are:

$$S_x^{\frac{3}{2}\frac{1}{2}} = \begin{pmatrix} 0 & \frac{1}{2} & 0 & 0 \\ \frac{1}{2} & 0 & 0 & 0 \\ 0 & 0 & 0 & 0 \\ 0 & 0 & 0 & 0 \end{pmatrix} S_y^{\frac{3}{2}\frac{1}{2}} = \begin{pmatrix} 0 & -\frac{i}{2} & 0 & 0 \\ \frac{i}{2} & 0 & 0 & 0 \\ 0 & 0 & 0 & 0 \\ 0 & 0 & 0 & 0 \end{pmatrix} S_z^{\frac{3}{2}\frac{1}{2}} = \begin{pmatrix} \frac{1}{2} & 0 & 0 & 0 \\ 0 & -\frac{1}{2} & 0 & 0 \\ 0 & 0 & 0 & 0 \\ 0 & 0 & 0 & 0 \end{pmatrix}$$

A general notation for the fictitious spin 1/2 operators can be defined:

$$S_x^{nm} \quad S_y^{nm} \quad S_z^{nm} \tag{1.42}$$

where n and m are the states of the allowed transition. With this formalism the propagators in equation (1.32) and the corresponding evolution of the density matrix from equation (1.28) can be calculated. These types of operators will be used in the last chapter to calculate the pulse sequences for the preparation of pure states and entanglement.

1.5.6 Basic Pulse Experiments

A $\pi/2$ pulse along the $x(y)$ axis rotates the equilibrium magnetization M_0 from z to the $+y(-x)$ axis, where it would stay indefinitely without dephasing or relaxation. In a real system there are always local inhomogeneities, which cause dephasing of the individual components of $M_{x,y}$ and after some time there is no net magnetization in the xy plane. Usually, the detection of pulsed ESR spectrometers is in this plane, and one obtains a time trace after the pulse that is called Free Induction Decay (FID). The Fourier transform of the FID gives the ESR spectrum [39]. The time trace for an on resonant y pulse of a single line spectrum is depicted in the Fig. (1.1). Using equation (1.36), the density matrix after a $\pi/2$ pulse is just:

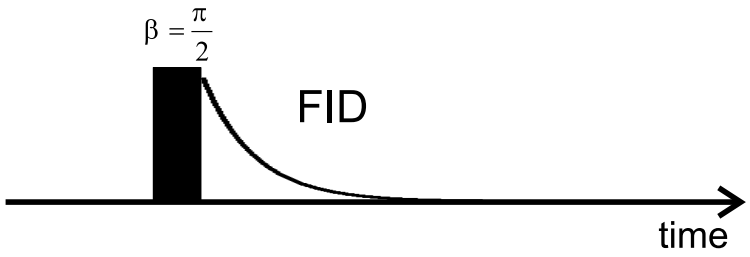

Fig. 1.1: Free Induction Decay (FID) after a $\pi/2$ pulse.

$$\rho_{FID} = |S_x) \tag{1.43}$$

The decay of the signal is proportional to $\exp(-\frac{t}{T_2^*})$ where T_2^* is the inhomogeneous spin-spin relaxation time. Comparing with equation (1.20) it is clear that broader lines will have shorter relaxation times and vice versa. Recalling the properties of the Fourier transformation, short pulses will also excite a larger spectral range and long pulses a narrower range.

The magnetization in the xy plane can be recovered (refocused) if an additional π pulse is applied at time τ after the first $\pi/2$ pulse. The magnetization is refocused at time 2τ (a phenomenon called Hahn echo after Erwin Hahn [42] who discovered it for nuclear spins). The pulse sequence is shown in Fig. (1.2). If the time between

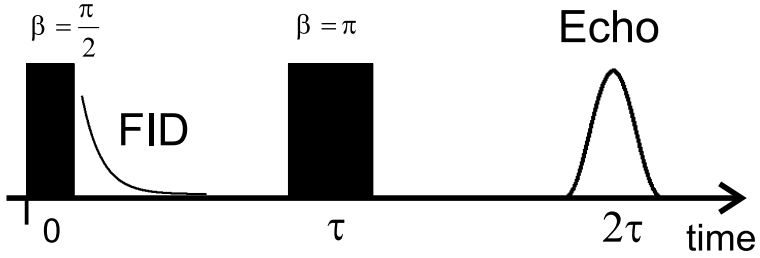

Fig. 1.2: Pulse sequence of the Hahn echo.

the pulses is increased, the echo signal decreases with $\exp(-\frac{2\tau}{T_2})$ where T_2 is the spin-spin relaxation time (sometimes called coherence time). Quantum mechanically, the action of the pulse sequence can be written using eqs. (1.35, 1.37) with the following propagator:

$$\hat{\hat{U}}_{echo} = e^{-\frac{i}{\hbar}\hat{\hat{H}}(t-\tau)} e^{-i\pi\hat{\hat{S}}_y} e^{-\frac{i}{\hbar}\hat{\hat{H}}\tau} e^{-i\frac{\pi}{2}\hat{\hat{S}}_y} \tag{1.44}$$

The density matrix after the pulse sequence is calculated for $\hat{\hat{H}} = \hbar\omega_0^i \hat{\hat{S}}_z$:

$$\rho(t) = \hat{\hat{S}}_y \cos\omega_0^i(t-\tau) - \hat{\hat{S}}_x \sin\omega_0^i(t-\tau) \tag{1.45}$$

where ω_S is the Larmor frequency of the electron spin i. The echo formation is governed by the line shape function. If the excited ESR line is symmetric, than the

first term will lead to an echo echo signal detection on the y-axis since the cosine is an even function. The odd sine function would not give a rise to an echo along the x-axis.
M_0 can be aligned along the $-z$ axis if a π pulse is applied. According to equation (1.36) then:

$$\rho_\pi = -|S_z) \tag{1.46}$$

The recovery of the magnetization to its equilibrium value is described by $\exp -(\frac{2\tau_1}{T_1})$ where T_1 is the spin-lattice relaxation time. An often used pulse sequence to measure T_1 is the inversion recovery shown in Fig. (1.3). Note that the Hahn echo pulse

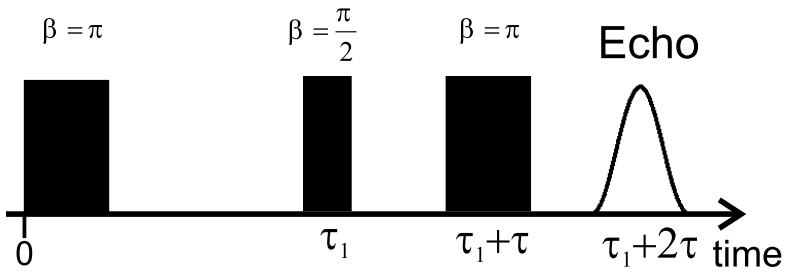

Fig. 1.3: Pulse sequence of the inversion recovery.

sequence is used here as a detector sequence, and that usually $\tau \ll \tau_1$ is kept constant throughout this experiment.

1.6 ENDOR

In a system of coupled electron and nuclear spin there will be not only ESR transitions but also ones between the nuclear spins. In order to fully explore the properties of such a coupled system a new method was developed called Electron Nuclear Double Resonance (ENDOR). It was discovered by Feher [43] who first observed nuclear transitions via electron spin resonance. This method is a very useful technique for obtaining NMR spectra for paramagnetic samples. Much less spin concentration is needed for an ESR experiment than for NMR because of the larger gyromagnetic ratio γ (for a free electron and a proton $\gamma_e = 1854\gamma_P$). Larger γ gives rise to larger spin polarization which rises the signal since the latter in magnetic resonance experiments is proportional to the population difference (polarization). The basic principles of ENDOR spectroscopy will be briefly discussed.
The simplest example is a system consisting of an electron spin 1/2 and a nuclear spin 1/2 with isotropic hyperfine interaction constant a in constant magnetic field. The energy diagram is shown in Fig. 1.4. The allowed ESR transitions are $|2\rangle \leftrightarrow |4\rangle$ (solid line) and $|1\rangle \leftrightarrow |3\rangle$ (dotted line), while $|1\rangle \leftrightarrow |2\rangle$ and $|3\rangle \leftrightarrow |4\rangle$ (dashed lines)

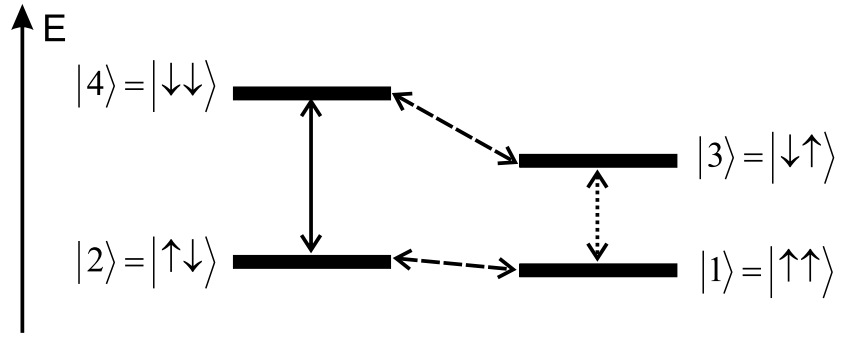

Fig. 1.4: Energy diagram for a system with $S = 1/2$ and $I = 1/2$.

are NMR transitions. As there is a Boltzmann distribution, states $|1\rangle$ and $|2\rangle$ will be more populated than $|3\rangle$ and $|4\rangle$. In order to obtain an ENDOR spectrum, first one of the two ESR transition is saturated. This can be realized either by continuous MW irradiation or by an application of one π (Davies ENDOR) or two $\pi/2$ (Mims ENDOR) MW pulses. The transition will stay saturated as long as the continuous radiation is on or for a time T_1 (the spin-lattice relaxation time) after the MW pulse(s). During that time a constant or pulsed radio frequency (RF) field is applied and the ESR signal strength is monitored. The RF frequency is swept around the resonance frequency of the NMR transition. When the RF is at resonance, there is a decay of the ESR signal, because there is a decrease in the population difference. For pulsed ENDOR a detection sequence is applied (after the RF pulse) in the form

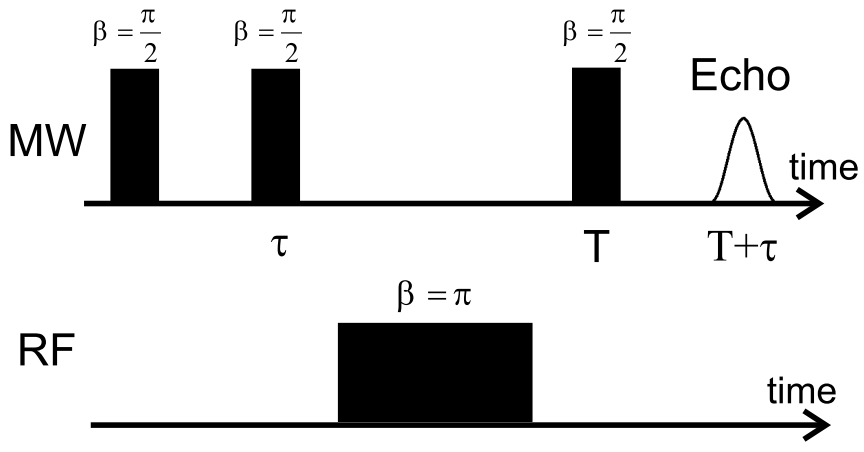

Fig. 1.5: Mims ENDOR pulse sequence.

of a $\pi/2$ MW pulse (Mims ENDOR) or a Hahn Echo (Davies ENDOR) sequence. The ENDOR RF frequency for this example can be calculated with:

$$\nu_{1,2} = \nu_L \pm \frac{1}{2}a \tag{1.47}$$

where $\nu_{1,2}$ are the two ENDOR transition frequencies, ν_L is the Larmor precession frequency of the nuclear spin and a is the hyperfine constant given in MHz. For an electron spin S and nuclear spin 1/2 (1.47) is:

$$\nu_{m_S} = \nu_L + m_s a \tag{1.48}$$

here m_s is the electron spin quantum number.
The pulse sequence for the Mims ENDOR experiment is shown in Fig. 1.5 as it will be used later in this work. The first two MW pulses invert the population difference of the desired ESR transition. The stimulated echo signal decreases when the RF pulse is at resonance. Mims ENDOR is easier to implement than Davies ENDOR, because for the latter the power of the first inverting MW pulse must be much larger than for the detection pulses [39].